Land-Use/Land-Cover Change Detection Using Improved Change-Vector Analysis

Jin Chen, Peng Gong, Chunyang He, Ruiliang Pu, and Peijun Shi

Abstract

*Change-vector analysis (*CVA*) is a valuable technique for land-use/land-cover change detection. However, how to reasonably determine thresholds of change magnitude and change direction is a bottleneck to its proper application. In this paper, a new method is proposed to improve* CVA*. The method (the improved* CVA*) consists of two stages, Double-Window Flexible Pace Search (*DFPS*), which aims at determining the threshold of change magnitude, and direction cosines of change vectors for determining change direction (category) that combines single-date image classification with a minimum-distance categorizing technique. When the improved* CVA *was applied to the detection of the land-use/land-cover changes in the Haidian District, Beijing, China, Kappa coefficients of "change/no-change" detection and "from-to" types of change detection were 0.87 and greater than 0.7, respectively, for all kinds of land-use changes. The experimental results indicate that the improved* CVA *has good potential in land-use/land-cover change detection.*

Introduction

Land-use/land-cover change is an important field in global environmental change research. Inventory and monitoring of land-use/land-cover changes are indispensable aspects for further understanding of change mechanism and modeling the impact of change on the environment and associated ecosystems at different scales (Turner *et al.*, 1995; William *et al.*, 1994). Remote sensing is a valuable data source from which land-use/land-cover change information can be extracted efficiently. In the past two decades, there has been a growing trend in the development of change detection techniques using remote sensing data. A number of techniques for accomplishing change detection using satellite imagery have been formulated, applied, and evaluated, which can be broadly grouped into two general types (Singh, 1989; Jensen, 1996; Coppin and Bauer, 1996; Ding *et al.*, 1998; Johnson and Kasischke, 1998): (1) those based on spectral classification of the input data such as post-classification comparison (e.g., Mas, 1999) and direct two-date classification (e.g., Li and Yeh, 1998); and (2) those based on radiometric change between different acquisition dates, including (a) image algebra methods such as band differencing (Weismiller *et al.*, 1977), ratioing (Howarth and Wickware, 1981), and vegetation indices (Nelson, 1983); (b) regression analysis (Singh, 1986); (c) principal component analysis (Byrne *et al.*, 1980; Gong, 1993); and (d) change-vector analysis (CVA) (Malila, 1980). Based on a mixture of categorical and radiometric change information, hybrid approaches have also been proposed and evaluated (Colwell and Weber, 1981). Selection of an appropriate change-detection technique, in practice, often depends on the requirement of information, data availability and quality, time and cost constraints, and analysis skill and experience (Johnson and Kasischke, 1998). Among those radiometric change-based approaches, change-vector analysis is a useful method for land-use/land-cover change detection because it not only can avoid the shortcomings of those type 1 approaches, such as cumulative error in image classification of an individual date, but also it can find changed pixels using more, even all, the bands and provide "from-to" type of change information. In the past few years, its advantages and potential have been demonstrated in some case studies (Michalek *et al.*, 1993; Lambin and Strahler, 1994a; Lambin and Strahler, 1994b; Sohl, 1999). Thus, it has recently been adopted as the basis for the initial 250-meter Land-Cover Change Product using MODIS Data (Zhan *et al.*, 2000).

However, like other radiometric change approaches, CVA also has several drawbacks that limit its use. These include

- *A strict requirement for reliable image radiometry.* Because CVA is based on pixel-wise radiometric comparison, the accuracy of image radiometric correction for alleviating the impacts caused by disturbing factors such as different atmospheric conditions, solar angle, soil moisture and vegetation phenology, etc., is more critical for CVA than for spectral classification approaches. However, there exists no valid radiometric correction method that can be used to reduce the effects of all disturbing factors efficiently, especially for vegetation phenology. Similar acquisition dates in different years are therefore chosen to reduce this type of disturbance in CVA. This strict requirement for data acquisition limits the broad application of CVA.
- *A lack of automatic or semiautomatic methods to effectively determine the threshold of change magnitude between change and no-change pixels.* Although determination of the optimal threshold between change and non-change pixels is considered as the most important task as well as the greatest challenge of CVA (Ding *et al*, 1998; Johnson and Kasischke, 1998; Smits and Annoni, 2000), the threshold in a specific CVA analysis is often determined according to empirical strategies (Fung and LeDrew, 1988) or from manual trial-and-error procedures. This usually requires a more experienced image analyst and a long trial time (Bruzzone and Prieto, 2000).
- *Discrimination of different phenomenological types of change is problematic when the number of bands involved is large.* The methods of discriminating change type in existing literature can be grouped into three classes: (1) trigonometric functions of vector angle in two spectral dimensions (Malila, 1980), (2)

J. Chen, C. He, and P. Shi are with the Key Laboratory of Environmental Change and Natural Disaster, Beijing Normal University, Ministry of Education of China, Beijing 100875, China.

P. Gong and R. Pu are with the International Institute for Earth System Science, Nanjing University, China; and the Center for Assessment and Monitoring of Forest and Environmental Resources, 145 Mulford Hall, University of California, Berkeley, CA 94720-3114 (gong@nature.berkeley.edu).

Photogrammetric Engineering & Remote Sensing
Vol. 69, No. 4, April 2003, pp. 369–379.

0099-1112/03/6904–369$3.00/0

sector coding in more than two spectral dimensions (Virag and Colwell, 1987), and (3) principal component analysis in a multitemporal space (Lambin and Strahler, 1994a). In most CVA applications, the change category is mainly distinguished and assigned by a combination of "+" or "−" symbols (+ for increase, (− for decrease) of each computational band and image interpretation (Virag and Colwell, 1987; Michalek *et al.*, 1993; Johnson and Kasischke, 1998; Sohl, 1999). When CVA is applied in this manner (called "sector coding"), there exist two problems. First, sector coding can discriminate 2^n sectors when the number of computational bands is n (Virag and Colwell, 1987). If there are nine land-cover types found at two different dates, respectively, and all kinds of changes between those land covers probably occur in the period, the number of change types is $9 \times 8 = 72$. This means that one sector code certainly represents more than one change type even if six bands of TM are used ($2^6 = 64$), which may lead to an assignment error of change category. Second, it is a strenuous and time-consuming work to discriminate and interpret change categories represented by sector codes with the increase of computational bands (n) because the number of sector codes increases geometrically.

In light of the abovementioned drawbacks, especially the second and third ones, this paper presents an improved CVA for land-use/land-cover change detection, which includes (1) a semiautomatic method, named Double-Window Flexible Pace Search (DFPS), which aims at determining efficiently the threshold of change magnitude, and (2) a new method of determining change direction (change category) which combines a single image classification and a minimum-distance categorization based upon the direction cosines of the change vector. The improved CVA approach is applied and validated by a case study of land-use change detection in the Haidian district of Beijing, China, using multi-temporal TM data. The rest of this paper outlines the proposed method and gives a detailed description of a case study applying the improved CVA. The conclusions and remarks are summarized.

Method

Change-Vector Analysis (CVA)

Malila (1980) gave a general idea of change-vector analysis (CVA). A change vector can be described by an angle of change (vector direction) and a magnitude of change from date 1 to date 2 (Jensen, 1996). If a pixel's gray-level values in two images on dates t_1, t_2 are given by $\mathbf{G} = (g_1, g_2, \cdots, g_n)^{\mathrm{T}}$ and $\mathbf{H} = (h_1, h_2, \ldots, h_n)^{\mathrm{T}}$, respectively, and n is the number of bands, a change vector is defined as

$$\Delta\mathbf{G} = \mathbf{H} - \mathbf{G} = \begin{pmatrix} h_1 - g_1 \\ h_2 - g_2 \\ \cdots \\ h_{\mathrm{n}} - g_{\mathrm{n}} \end{pmatrix} \tag{1}$$

where $\Delta\mathbf{G}$ includes all the change information between the two dates for a given pixel, and the change magnitude $\|\Delta G\|$ is computed with

$$\|\Delta G\| = \sqrt{(h_1 - g_1)^2 + (h_2 - g_2)^2 + \cdots + (h_n - g_n)^2}. \tag{2}$$

It represents the total gray-level difference between two dates. The greater $\|\Delta G\|$ is, the higher is the possibility of change. A decision on change is made based on whether the change magnitude exceeds a specific threshold. Once a pixel is identified as change, the direction of $\Delta\mathbf{G}$ can be examined further to determine the type of change. The type of change is often identified using the angle of the vector in two spectral dimensions, or sector codes if more than two spectral dimensions are involved. The geometric concept of CVA is applicable to any number of spectral bands, no matter what measurement scale of radiance is used. Based on the above introduction of CVA and its drawbacks, an improved CVA for land-use/land-cover change detection was developed (Figure 1).

Threshold Search for Identifying Change Pixels

Traditionally, the threshold of change magnitude is empirically determined. This is subjective and varies from person to person. To overcome this problem, we developed a Double-Window Flexible Pace Search (DFPS) algorithm. This method is based on selecting a threshold from training samples containing all possible kinds of changes. The assumption is that the training samples are representative to the entire study area. Thus, a threshold leading to the maximum accuracy of change detection within the training samples is considered optimal for the entire study area. The flowchart of DFPS is shown in Figure 2 and its main steps are described in the following section.

Selection of Typical Sample Areas of Land-Use/Land-Cover Change

In the process of optimal threshold search, it is important to make sure that training samples are as representative as possible for all change classes. First, the change magnitude ($\|\Delta G\|$) image is calculated from the two original images of different dates, following precise image-to-image registration and radiometric normalization. Then, some typical change areas are chosen as training samples from the change magnitude image. The two original images can be displayed along with the change magnitude image to assist in the identification of training samples for land-use changes. The criteria for selecting sample areas are (1) training samples should cover as many as possible change types (note that a change type is identified only by comparing the color and context between the two original images because the real change type has not been categorized at this stage), (2) training samples should include only change pixels,

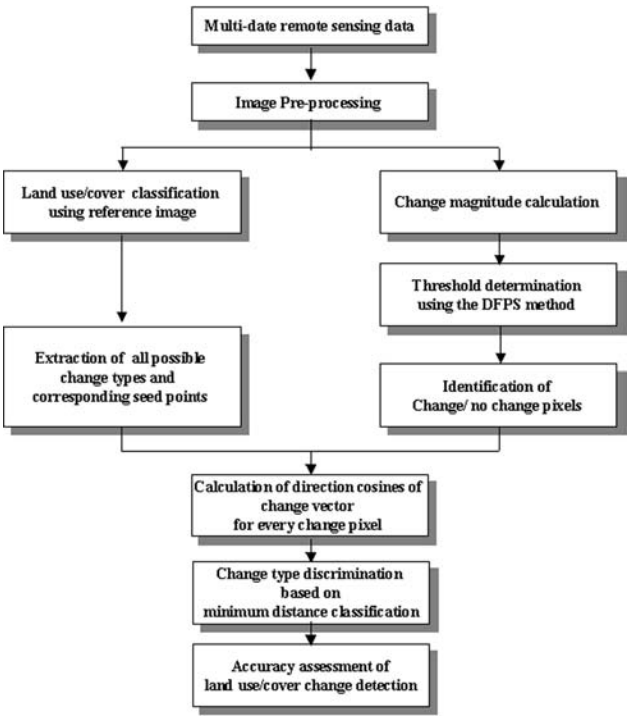

Figure 1. Flowchart of land-use/land-cover change detection based on improved change vector analysis.

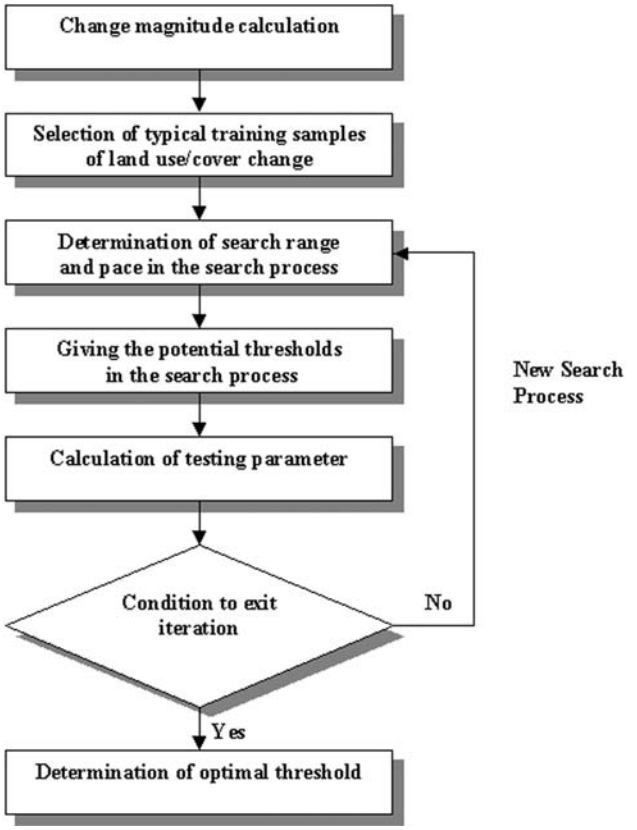

Figure 2. Flowchart of the Double-windows Flexible Pace Search method.

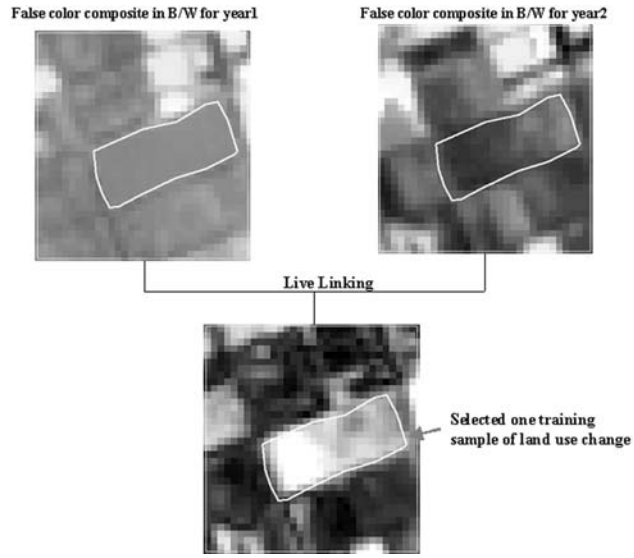

Figure 3. An example of selecting a training patch in the change magnitude image by comparing the two original images.

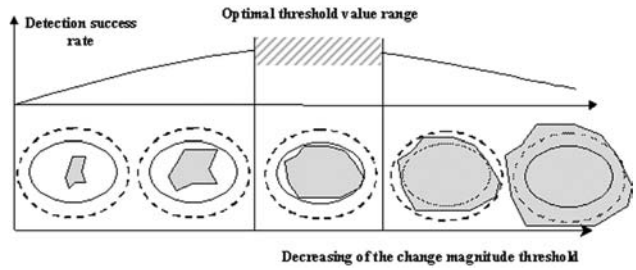

Figure 4. An example showing the relationship between accuracy of change detection and threshold decreasing in one training sample. The shadow area corresponds to an optimal threshold value.

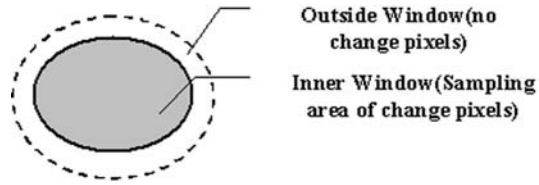

Figure 5. Example of Double-window.

and (3) training samples should be encircled by no-change pixels as "islands." Figure 3 shows an example of selecting one training sample in the change magnitude image by comparing the two original images.

The threshold for identifying change and no-change pixels can be determined by searching an optimal value of change magnitude to obtain the maximum accuracy of change detection within the training samples. Obviously, as the threshold of change magnitude decreases, the number of change pixels inside training samples will increase and the accuracy of change detection will be improved. However, it should be noted that the possibility of no-change pixels outside the training samples identified as change pixels would also increase, leading to higher commission errors. There exists such a threshold, with which all the pixels inside the training samples are detected correctly as change pixels and the highest accuracy is obtained in the training samples while many no-change pixels outside the training samples are also identified incorrectly as change pixels. Figure 4 gives an example illustrating the relationship between accuracy of change detection and threshold decrease in one training patch. In consideration of this situation, an outside boundary is created through buffering in a GIS for each training patch, forming a double area called a double-window (Figure 5). The outside boundary (outside window) is used to prevent the threshold from being too low.

Determination of the Search Range and Pace

The threshold search range can be set as a difference between the minimum value (a) and the maximum value (b) of change magnitude in the first search process. The first search pace (increment) P_1 may be calculated according to the following formula:

$$P_1 = (b - a)/\, m \tag{3}$$

where m is a positive integer, which determines the number of

potential thresholds in a search process and can be set manually. The potential thresholds to detect change pixels from the training samples in the search process are given within the range of $[a, b]$ as $b - P_1, b - 2P_1, \ldots$. It should be noted that the size of the manually set m does not affect the search efficiency and the final results. A large m increases the number of potential thresholds during one search, but it decreases the number of searches.

Definition and Calculation of Test Parameter

A success rate of change detection is defined to evaluate the performance of each potential threshold during one search process for identifying change/no-change pixels. The success rate (L_k) is calculated for a potential threshold of k: i.e.,

$$L_k = \frac{(A_{k1} - A_{k2}) \times 100}{A} \% \tag{4}$$

where A_{k1} is the number of change pixels detected inside all training patches (in the inner windows), A_{k2} is the number of change pixels which are detected incorrectly in the outside boundary of all training patches (in the outside windows), and A is the total number of pixels within all training patches (in the inner windows). In order to keep L_k from becoming negative, the outside border (outside window) should be set to one or two pixels for each training sample. From this definition, it can be seen that the double-window concept is useful in controlling the commission error caused by low thresholds, because low thresholds increases A_{k2} and reduces L_k.

After all L_k for all m thresholds in one search are obtained, the maximum and minimum values of L_k can be found and designated as $L_{\max}$ and $L_{\min}$ during this search process. If the two parameters do not satisfy the conditions described in the next section, a new search begins, the new search range is set in the range $[k_{\max} - P_1, k_{\max} + P_1]$, and a new smaller search pace is set based on the modified search range with Equation 3. Here, $k_{\max}$ is the potential threshold value corresponding to $L_{\max}$ in the search process.

Condition to Exit the Iteration

The steps described in the previous two sections represent an iterating process, which will terminate when the following formula is satisfied:

$$L_{\max} - L_{\min} \leq \delta \tag{5}$$

where $L_{\max}$ and $L_{\min}$ are the maximum and minimum values of the success rate in one search process, and δ is an acceptable error constant. The condition indicates that the change of search pace has little influence on the result of change/no-change pixel detection. The threshold corresponding to $L_{\max}$ is considered as an optimal threshold for change detection.

The method of Double-Window Flexible Pace Search (DFPS) is a semiautomatic method for determining the optimal threshold of change detection that only requires the involvement of the image analyst during the selection of typical training samples of land-use/land-cover change. The advantages of this method can be summarized as (1) the optimal threshold can be obtained automatically after the selection of typical training samples of land-use/land-cover change, (2) the commission error caused by over decreasing the threshold can be controlled effectively through the double-window technique, and (3) search efficiency is improved with the flexible and varied search pace. Although the new method may perform better compared with some previous empirical methods, it should be noted that the new method is dependent on training samples, which to a certain degree relies on the experience and skills of the image analyst.

Change Type Discrimination

Discrimination of change types plays an important role in change detection. Problems were noted with the existing CVA (Cohen and Fiorella, 1998). Cohen and Fiorella (1998) pointed out the possibility of other angle measurements for the change vector in three or more spectral dimensions and noticed the importance of a "reference image" in change-type discrimination. A new method of determining change type (category) is developed in this study, which combines single image classification (as a reference image) with minimum-distance categorizing based on direction cosines of change vectors.

The direction of a vector can be described by a series of cosine functions in a multi-dimensional space. This series is called direction cosines (Hoffmann, 1975). The direction of the change vector containing change type information can also be defined by the cosine function of angles between the vector and each spectral axis. The change vector direction of one change pixel corresponds to one and only one point in a multi-dimensional space constituted by direction cosines. If some typical feature points (hereafter called seed points) and their corresponding change types in the space of direction cosines are known, the change type of a change pixel can be determined by a supervised classification on the basis of its proximity to those seed points. Obviously, to obtain seed points and their corresponding change types becomes the key to change-type discrimination for all change pixels. For two images acquired on different dates t_1 and t_2, after rigorous radiometric normalization, we may assume that the spectral feature difference between any two kinds of land-use/land-cover types on either date are similar to their spectral change features from t_1 to t_2. With this assumption, we can first carry out a land-use/land-cover classification from the image of a selected date, either t_1 or t_2 (the reference image). This reference image should be the one with more ancillary information available for accurate image classification. The spectral difference vectors between any two land-use/land-cover types in the reference image can then be calculated based on the classified land-use/land-cover types and transplanted into the direction cosine space. These points can be considered as the seed points (mean vectors) in a minimum-distance classification for land-use/land-cover change-type discrimination because their features are typical and their coordinates and change types are known.

Definition of Direction Cosines of Change Vector

Suppose $\mathbf{X}(x_1, x_2, x_3, \ldots, x_n)$ is an n dimensional vector, its magnitude can be calculated as

$$|\mathbf{X}| = \sqrt{x_1^2 + x_2^2 + x_3^2 + x_4^2 + \cdots + x_n^2}. \tag{6}$$

If the angles between $\mathbf{X}$ and each axis are $(\theta_1, \theta_2, \theta_3, \theta_4, \ldots, \theta_n)$, respectively, then its direction can be described by cosine functions of these angles as (Hoffmann, 1975)

$$\cos\,\theta_1 = \frac{x_1}{|\mathbf{X}|}, \cos\,\theta_2 = \frac{x_2}{|\mathbf{X}|}, \ldots, \cos\,\theta_n = \frac{x_n}{|\mathbf{X}|} \tag{7}$$

Using Equation 7, the direction of a change vector can be represented as one and only one point, defined as a new vector $\mathbf{Z}(\cos\theta_1, \cos\theta_2, \cos\theta_3, \ldots, \cos\theta_n)$ in the direction cosine space. All of the change pixels have their corresponding points in this space. According to this definition, the determination of change types is turned into a classification problem of points in the direction cosine space. Moreover, using the direction cosines instead of angle measurements can avoid the difficulty of "baseline" establishment for angle measurement such as using Tasseled-cap transformation to build the Plane of Soil (defined by brightness and wetness axes) and Vegetation (defined by brightness and greenness axes) (Crist and Cicone, 1984).

Extraction of all Possible Change Types and Their Corresponding Seed Points

For two images acquired on different dates t_1 and t_2, after rigorous radiometric normalization, the spectral feature differences between any two kinds of land-use/land-cover types on either date are similar to their spectral change features from t_1 to t_2. This assumption can be denoted as

$$\Delta \mathbf{W}_{ij} = \mathbf{P}_j - \mathbf{Q}_i \Leftrightarrow \Delta \mathbf{T}_{ij} = \mathbf{H}_j - \mathbf{G}_i \quad (8)$$

where $\mathbf{P}_j$ and $\mathbf{Q}_i$ are gray value vectors of land-use/land-cover types j and i in either image of date t_1 or t_2, $\Delta \mathbf{W}_{ij}$ is their spectral difference vector, $\mathbf{G}_i$ and $\mathbf{H}_j$ are gray-level vectors of land-use/land-cover types i and j at different dates t_1 and t_2, and $\Delta \mathbf{T}_{ij}$ is spectral change vector from date t_1 to t_2 (the same as the change vector as described above). Based on the land-use/land-cover classification from the reference image, the spectral difference vectors between any two kinds of land-use/land-cover types in the reference image are calculated. Using Equation 8, these spectral difference vectors can be thought of as equivalents of spectral change vectors of those land-use/land-cover changes from date t_1 to t_2. The mean of spectral difference vectors represents a typical feature of various changes between any two kinds of land-use/land-cover types, and direction cosine values of the mean of spectral difference vectors can be specified as seed points in the direction cosine space. Moreover, the standard deviation of spectral difference vectors that belong to the same type of land-use/land-cover change can also be used to determine the threshold of an unclassified class in a minimum-distance classifier.

The mean of spectral difference vectors and their standard deviations can be calculated based on change samples in a particular "from i to j" change class with an assumption that the probability distributions of spectral differences are normal. This is usually possible because each spectral class (land-use/land-cover class) is usually normally distributed in the spectral space (this is the same assumption used in a maximum-likelihood classification; Richards and Jia, 1999). We used $\mathbf{EX}_i$, $\mathbf{DX}_i$, $\mathbf{EX}_j$, and $\mathbf{DX}_j$ to denote the mean and standard deviation vectors of land-use/land-cover types i and j in multispectral space (n bands), respectively: i.e.,

$$\mathbf{EX}_i = (EX_{i1}, EX_{i2}, ..., EX_{in})^{\mathrm{T}} \quad (9)$$

$$\mathbf{DX}_i = (DX_i, DX_{i2}, ..., DX_{in})^{\mathrm{T}} \quad (10)$$

$$\mathbf{EX}_j = (EX_{j1}, EX_{j2}, ..., EX_{jn})^{\mathrm{T}} \quad (11)$$

$$\mathbf{DX}_j = (DX_j, DX_{j2}, ..., DX_{jn})^{\mathrm{T}} \quad (12)$$

Based on stochastic theory, if p and q are mutually independent and subject to a normal distribution, then $z = p - q$ is also subject to a normal distribution. Thus, the mean and the standard deviation of spectral difference vector of land-use/land-cover types j and i can be simply deduced from $\mathbf{EX}_i$, $\mathbf{DX}_i$, $\mathbf{EX}_j$, and $\mathbf{DX}_j$ as follows:

$$\mathbf{EX}_{ij} = (EX_{j1} - EX_{i1}, EX_{j2} - EX_{i2}, ..., EX_{jn} - EX_{in})^{\mathrm{T}} \quad (13)$$

$$\mathbf{DX}_{ij} = (DX_{j1} + DX_{i1}, DX_{j2} + DX_{i2}, ..., DX_{jn} + DX_{in})^{\mathrm{T}} \quad (14)$$

Change-Type Discrimination Based on Minimum-Distance Classification

Types of change pixels can be discriminated by classifying direction cosines of their change vectors. As described in the previous section, the mean and the standard deviation vectors of each land-use/land-cover change type can be obtained from the reference image without strenuous and time-consuming training work. Thus, the minimum-distance classifier was selected for this study to identify land-use/land-cover change types based on its effectiveness and its simple requirement of only the estimation of the mean vector of each spectral class (Richards and Jia, 1999). With this classifier, an unknown pixel is assigned to a certain class or unclassified class based on a minimum distance to means of all candidate classes when the distance is within a certain threshold. The minimum-distance classifier was employed in this study to categorize change types in three steps: (1) calculating direction cosines of the spectral change vector for each change pixel according to Equation 7; (2) calculating Euclidean distances of the changed pixels to seed points corresponding to all possible change types in the direction cosine space, and those seed points are obtained through land-use/land-cover classification in a reference image; and (3) determining change types of land-use/land-cover by applying the minimum-distance rule. Like a conventional minimum-distance classifier, the unclassified pixels are those falling outside the threshold range based on the mean and standard deviation of every class. Those pixels may stand for new change types, which are not included in all possible change types obtained through land-use/land-cover classification in the reference image.

Case Study—Land-Use Change Detection in the Haidian District, Beijing, China

Study Area and Data

The Haidian district (one district of the city of Beijing) is located in the west and northwest part of Beijing with a population of 1.25 million and an area of 426 km^2 (Figure 6). Three-quarters of the district lie in a plain with an elevation of less than 50 meters, while hills cover the remaining quarter of the district. It is an educational and cultural center, a vegetable production area for Beijing, and a famous Information Technology (IT) industrial area of China. With a rapid growth in the economy during the past 20 years, tremendous land-use/land-cover

Figure 6. The study area (shadow area) in Beijing.

changes have taken place during this period. The area was selected as a study area to evaluate the performance of the improved CVA approach. In order to eliminate the effects of disturbance factors, especially vegetation phenological differences, two scenes of Landsat TM image data (path/row: 123/32, 06 May 1991 and 16 May 1997) covering the whole study area with good image quality were collected and used. Moreover, some auxiliary data were also collected, including 1:50,000-scale topographic maps from 1972, a 1:100,000-scale land-use map from 1991, GPS survey data from 1999, and a SPOT panchromatic image from May 1997.

Image Prepreprocessing

Geometric Registration

High precision geometric registration of the multi-temporal image data is a basic requirement for change detection (Gong *et al.*, 1992; Dai and Khorram, 1998; Morisette and Khorram, 2000). First, the 1991 TM image was transformed to the UTM projection at a 30- by 30-m resolution, using second-order polynomial and bilinear interpolation. Twenty-one ground control points were collected from the 1:50,000-scale topographic maps. The root-mean-square error (RMSE) was less than 1 pixel. Then the 1997 TM image was registered to the 1991 image by image-to-image registration with an RMSE of registration of less than 0.5 pixels using 29 tie points. Finally, the boundary of the Haidian district, digitized into a GIS database, was used to clip the study area from the images.

Image Radiometric Normalization

A problem associated with the use of multi-temporal remote sensing data for change detection is that the multi-temporal data are usually acquired under different sun angle, and atmospheric and soil moisture conditions. Ideally, such data should be radiometrically normalized so that the effects of those undesirable conditions can be minimized or eliminated, which is critical to change detection, especially to those methods based on radiometric change (Hall *et al.*, 1991; Jensen *et al.*, 1995). In this study, the 1991 image was chosen as a primary reference image because the detailed ground reference information was available in that year. Then a Scattergram Controlled Regression (SCR) method was used to develop the radiometric normalization equations ($y_k = a_k x_k + b_k$) (Table 1) (Elvidge *et al.*, 1995). Here the independent variable x is the pixel values of the 1997 TM image while the dependent variable y is the normalized pixel values of the 1997 TM image. The R^2 of equations for most bands were greater than 0.95 except for band 2 with an R^2 of 0.88. Such equations were applied to normalize the 1997 image to assure that the images from 1991 and 1997 were comparable in terms of radiometric characteristics.

Change/No-Change Pixel Detection

Change Magnitude Calculation

Bands 1, 2, 3, 4, 5, and 7 of the TM 1991 image and TM 1997 image were used in the CVA analysis. According to Equations 1 and 2, change magnitudes between 1991 and 1997 were calculated and shown in Figure 7. The change magnitudes range from 0 to 177 (Figure 7b) and most change magnitudes fall under 100. From Figure 7a, it is obvious that greater values occur in the north part of the image.

TABLE 1. PARAMETERS USED FOR RADIOMETRIC NORMALIZATION FOR 1997 TM IMAGE

Band	Slope (a)	Intercept (b)	R^2
1	0.780	4.705	0.953
2	0.786	2.380	0.882
3	0.759	−1.40	0.959
4	0.791	2.491	0.959
5	0.648	11.669	0.981
7	0.808	−2.325	0.991

Threshold Determination Using the Double-Window Flexible Pace Search Method

Based on a preliminary comparison of the two images and interpretation, typical training samples of changes were selected with their 1-pixel outer buffer boundaries (some of the bigger ones shown in Plate 1a). Then the search range was set to [0, 180] and the pace as 20 initially. The Double-Window Flexible Pace Search method was used to determine the threshold of change magnitude. The threshold search process iterated until the success rate difference between the maximum and the minimum value was less than 0.1 percent. As a result, the threshold of change magnitude was obtained as 33.4 with a success rate of 63.78 percent. The search process was recorded in Table 2, and the search range changed five times with the paces of 20, 5, 1, 0.5, and 0.1. The number of thresholds tested totaled 36. The change pixels in the study area at threshold 33.4 were extracted and shown in Plate 1b.

Change Type Discrimination

Land-Use Classification Using the 1991 TM Image

Referring to the land-use map of 1991 and the results of the unsupervised classification of the 1991 TM image, all land classes in the study area were grouped into nine classes: urban land, barren land (mostly are transitional areas), water, paddy field, wheat land, vegetable land, other agricultural land, shrub and grassland, and forest land. Based on this classification system, a land-use/land-cover classification of the 1991 TM image (reference image) was carried out using the maximum-likelihood classifier and, after postpreprocessing (Plate 1a), an overall accuracy of 89 percent and a Kappa coefficient of 0.82 were reached.

Change-Type Discrimination

Based on the results of the land-use/land-cover classification of the 1991 TM image, the mean and standard deviation of each land-use/land-cover type were first extracted. Then the means of spectral difference vectors between any two kinds of land-use/land-cover types and their deviations were also calculated. There were 72 (9×8) possible land-use/land-cover change types in the study area. The program of change-type discrimination was performed nine times, respectively, using the change pixel data belonging to the nine land-use/land-cover types in 1991, and the change types of all change pixels were labeled, including a new type of unclassified class. By imposing the land-use/land-cover change image, including change pixels and change types, on the land-use image classified from the 1991 TM image, the land-use/land-cover image of 1997 was obtained and is shown in Plate 1d. Only 4 percent of the change pixels labeled as unclassified fell outside the threshold range of mean ± 2 times the standard deviation for each class. This suggests that a few new change types had occurred during this period, which were not included in all possible change types obtained through land-use/land-cover classification in 1991.

Comparing the land classification images in 1991 with 1997 (Plates 1c and 1d), the changes in the study area during this period may be characterized by two aspects. (1) Land-use changes within agricultural sectors took place notably in the north and northwest area, especially from other agricultural land changed to water pools, which were used mostly as fishponds. These changes resulted from increasing urban population and the rising living standard of city dwellers. (2) Urban

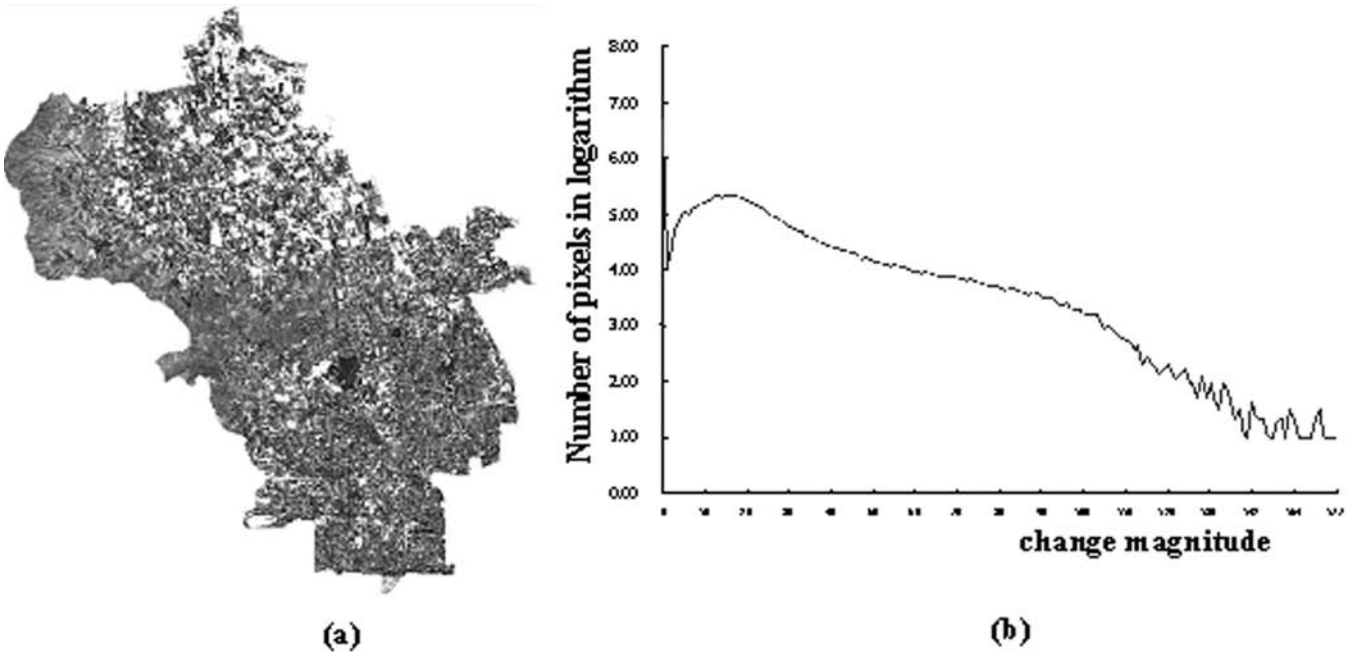

Figure 7. Change magnitude between 1991 and 1997 in the Haidian District, Beijing. (a) Change magnitude distribution. (b) Histogram of change magnitudes.

land expanded quickly in the urban-rural fringe area and the northern study area by encroaching upon agricultural land, especially paddy field and vegetable land and other agricultural lands, as a result of economic development.

Accuracy Assessment

In order to evaluate the performance of the proposed improved CVA method, the accuracy of change detection was estimated at both "change/no-change" detection and "from-to change" detection levels. This is different from a conventional accuracy assessment method that applies only to change detection errors (Khorram *et al.*, 1998; Biging *et al.*, 1998). At the "change/no-change" detection level, a random sampling technique was used. Because change pixels only occupy a small proportion of the image, the number of sampling pixels belonging to no-change were much more than that of change pixels. Table 3 shows an error matrix of "change/no-change" detection constructed from 2,400 sample pixels together with the auxiliary information visually interpreted from the 1997 image and SPOT panchromatic image of May 1997. A Kappa coefficient of 0.87 and an overall accuracy of 96.3 percent were achieved.

At the "from-to change" detection level, the accuracy assessment was carried out based on those change pixels belonging to different land-use/land-cover types in 1991. The sampling pixels used for accuracy assessment were selected using the randomly stratified sampling method, in which the detected change pixels (Figure 7b) were used for stratification. More than 60 samples were selected for each land-use/land-cover type in 1991 according to Congalton (1991). The ground truth was produced from visual interpretation of the1997 image and a SPOT panchromatic image acquired in May 1997. Table 4 shows the change-detection error matrix from wheat land in 1991 to other land-use types in 1997 as an example of all other change-detection error matrixes. Table 5 gives the accuracy assessment of the "from-to change" detection for all kinds of change types. It indicates that the proposed method is effective for change-type discrimination because the kappa coefficients for all kinds of change types exceeded 0.7.

In order to show the superiority of the improved CVA proposed in this paper, it is necessary to compare this method with other change-detection methods. Because the traditional CVA is computation intensive and is dependent on the user's experiences to a certain extent (to select the threshold and interpret change types), it was not used for comparison in this study. A comparison between the improved CVA and post-classification comparison, which is the most widely used method in change detection, was carried out. The post-classification comparison was performed based on a supervised classification using the 1991 and 1997 images, respectively, and the 1991 training data. At the "change/no-change" detection level, Table 6 gives the error matrix of post-classification comparison based on the same 2,400 sample pixels together with the auxiliary information also used in the improved CVA. It can be seen that the post-classification comparison causes an overestimation of change due to the cumulative errors of classification on each individual date. For example, 118 unchanged pixels (only 32 in the improved CVA) have been assigned to change in post-classification comparison. A comparison of Table 3 and Table 6 indicates that the improved CVA is better than the conventional method at the "change/no-change" detection level (the kappa coefficient is 0.87 for the improved CVA and 0.69 for post-classification comparison). Table 7 gives the accuracy assessment of the "from-to change" detection for all kinds of change types using the post-classification comparison. The same sample pixels in Table 5 were used to construct error matrices and calculate accuracies. It is evident that the post-classification comparison is more problematic than the improved CVA in almost every change type because a lot of unlikely land-use conversions and overestimation of change were produced from cumulative classification errors. The above results suggest that the improved CVA is effective and applicable for land-use/land-cover change detection.

Conclusion and Discussion

In this paper, we report some improvements made to the traditional change vector analysis in two aspects, determination of

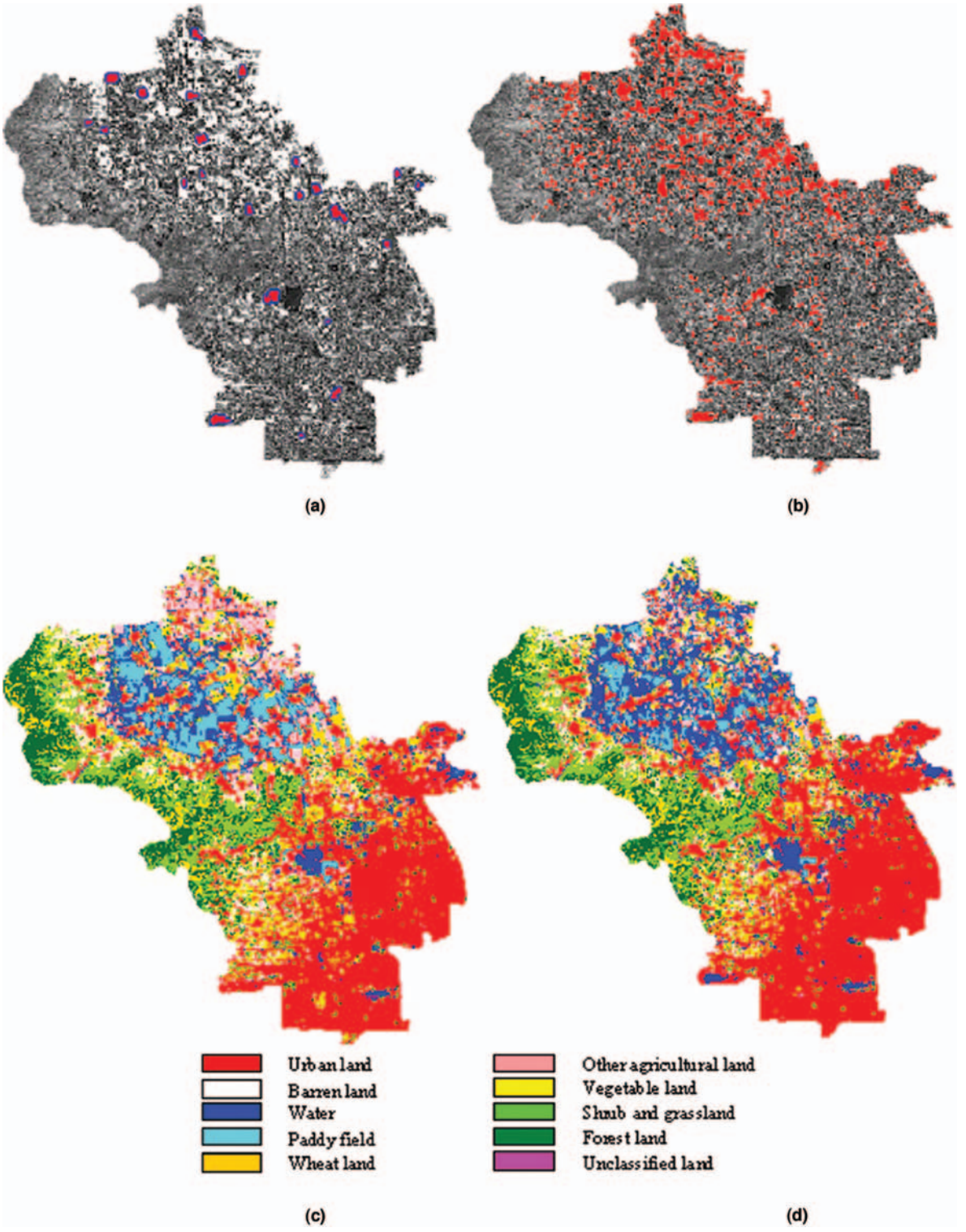

Plate 1. The selected change sample areas and results of change/no-change detection. (a) Typical change sample areas (red) with outer no-change buffer boundary (blue). (b) Change pixels detected by the improved CVA method. Land-use maps of the Haidian District, generated (c) by the maximum-likelihood classifier using the 1991 TM image, and (d) by the improved CVA with the 1997 TM image.

TABLE 2. RESULTS OF DOUBLE-WINDOW FLEXIBLE PACE SEARCH

Range 160-20 Pace 20		Range 60-20 Pace 5		Range 40-30 Pace 1		Range 35-33 Pace 0.5		Range 34-33 Pace 0.1	
Threshold	Success Rate	Threshold	Success Rate	Threshold	Success Rate	Threshold	Success Rate	Threshold	Success Rate
160	0.21	55	51.35	39	62.88	34.5	63.73	33.9	63.76
140	0.65	50	55.6	38	63.14	34	63.75	33.8	63.77
120	1.88	45	59.36	37	63.24	33.5	63.77	33.7	63.77
100	8.13	40	62.25	36	63.43			33.6	63.77
80	22.69	35	63.75	35	63.67			33.5	63.77
60	46.07	30	62.76	34	63.75			33.4	63.78
40	62.25	25	60.4	33	63.68			33.3	63.75
20	55.73			32	63.24			33.2	63.72
				31	62.65			33.1	63.69

TABLE 3. ERROR MATRIX FOR "CHANGE/NO-CHANGE" DETECTION USING THE IMPROVED CVA

		Reference Change			
		Change Pixels	No-Change Pixels	Sum	Commission Error
Classified Change	Change Pixels	368	32	400	8%
	No-Change Pixels	57	1943	2000	2.85%
	Sum	425	1975	2400	
	Omission Error	13.4%	1.6%		
	Overall Accuracy = 96.29% Kappa Coefficient = 0.8698				

TABLE 4. CHANGE DETECTION ERROR MATRIX FROM WHEAT LAND IN 1991 TO OTHER TYPES IN 1997 USING THE IMPROVED CVA

		Reference Change								
		Wheat Land								
	1991	1997	Urban Land	Barren Land	Water	Paddy Field	Other Agricultural Land	Vegetable Land	Shrub and Grassland	Forest Land	Sum
Classified Change	Wheat Land	Urban Land	**13**					1			14
		Barren Land	2	**20**			1				23
		Water			**12**	2					14
		Paddy Field			3	**20**			1		24
		Other Agricultural Land									0
		Vegetable Land	4					**11**			15
		Shrub and Grassland							**7**		7
		Forest Land								**1**	1
		Sum	19	20	15	22	1	12	8	1	98
	Overall Accuracy = 85.71% Kappa Coefficient = 0.8264										

TABLE 5. THE ACCURACY ASSESSMENT OF "FROM-TO" CHANGE DETECTION USING THE IMPROVED CVA

Land Use in 1991	Land Use in 1997	Sampling Pixels	Overall Accuracy	Kappa Coefficient
Urban Land	Other Land-Use Types	60	84.56	0.7156
Barren Land		90	87.33	0.838
Water		80	92.86	0.8401
Paddy Field		90	81.36	0.7796
Other Agricultural Land		90	86.72	0.8108
Wheat Land		98	85.71	0.8264
Vegetable Land		90	89.04	0.8516
Shrub and Grassland		90	92.05	0.8668
Forest Land		90	85.71	0.7456

the threshold of change magnitude and change type discrimination. When the improved method was employed for the Haidian District, Beijing with Landsat TM imagery acquired in 1991 and 1997, the Kappa coefficients of "change/no-change" detection and "from-to change" detection were 0.87 and greater than 0.7, respectively, for all kinds of change types. The results suggest that the improved CVA is effective and has potential in land-use/land-cover change detection.

Good data quality (similar acquisition dates in different years and cloud-free) and image radiometric normalization

TABLE 6. ERROR MATRIX FOR "CHANGE/NO-CHANGE" DETECTION USING POST-CLASSIFICATION COMPARISON

		Reference Change			
		Change Pixels	No-Change Pixels	Sum	Commission Error
Classified Change	Change Pixels	321	118	439	26.88
	No-Change Pixels	104	1857	1961	5.30
	Sum	425	1975	2400	
	Omission Error	24.47	5.97		
	Overall Accuracy = 90.75% Kappa Coefficient = 0.6867				

TABLE 7. THE ACCURACY ASSESSMENT OF "FROM-TO" CHANGE DETECTION USING POST-CLASSIFICATION COMPARISON

1991	1997	Sample Pixels	Overall Accuracy	Kappa Coefficient
Urban Land	Other Land-Use Types	60	62.15	0.4923
Barren Land		90	76.37	0.6421
Water		80	86.91	0.7902
Paddy Field		90	74.24	0.6332
Other Agricultural Land		90	81.23	0.7216
Wheat Land		98	79.24	0.681
Vegetable Land		90	69.32	0.5637
Shrub and Grassland		90	73.47	0.5718
Forest Land		90	73.25	0.5689

have a strong impact on the final change-detection result because the proposed method is based on an assumption of radiometric similarity among multi-temporal remotely sensed data. In addition, the selection of typical change sample areas and single-image classification are also critical to the search of an optimal threshold of change magnitude and identification of change types. In our study, thanks to the good quality of image data, rigorous radiometric and geometric correction, and rich ancillary materials, relatively satisfactory results were obtained. However, desirable imaging conditions are not always guaranteed; therefore, the change-detection accuracy of the improved CVA approach may decrease.

In most land-use/land-cover change-detection applications, collection of rich ancillary information in all years is usually difficult. This may lead to error accumulation due to unreliable classification of images from all dates. The new method of determining change type developed in this paper takes advantage of the spectral differences between images acquired in two dates t_1 to t_2, and the rich ancillary information from one date for classification for reference. It is based on two assumptions: (1) the direction cosine of the change vector contains change type information, and (2) the spectral feature difference between any two kinds of land-use/land-cover types on either date are similar to their spectral change features from t_1 to t_2. If these assumptions are reasonable, no ancillary information from another date is needed to perform change type discrimination. Although we need some ancillary reference data on change to evaluate the change detection result, in practice, this requirement is much less than in other change-detection methods. The improved CVA is an effective approach, especially when ancillary information for classification is only available on one date.

Acknowledgments

This research was partially supported by the National Basic Science Program of China (2001CB309404), and NASA's land-cover and land-use change grants (NAG5-9231; NCC5-492).

References

Biging, Gregory S., David R. Colby, and Russell G. Congalton, 1998. Sampling system for change detection accuracy assessment, *Remote Sensing Change Detection: Environmental Monitoring Methods and Applications* (Ross S. Lunetta and Christopher D. Elvidge, editors), Sleeping Bear Press, Inc., New York, N.Y., pp.281–308.

Bruzzone, L., and D.F. Prieto, 2000. Automatic analysis of the difference image for unsupervised change detection, *IEEE Transactions on Geoscience and Remote Sensing*, 38(3):1171–1182.

Byrne, G.F., P.F. Crapper, and K.K. Mayo, 1980. Monotoring land-cover by principal component analysis of multitemporal Landsat data, *Remote Sensing of Environment*, 10:175–184.

Cohen, W.B., and M. Fiorella, 1998. Comparison of methods for detecting conifer forest change with Thematic Mapper imagery, *Remote Sensing Change Detection: Environmental Monitoring Methods and Applications* (Ross S. Lunetta and Christopher D. Elvidge, editors), Sleeping Bear Press, Inc,, New York, N.Y., pp. 89–102.

Colwell, J., and F. Weber, 1981. Forest change detection, *Fifteenth International Symposium on Remote Sensing of Environment*, 11-15 May, Ann Arbor, Michigan, pp. 65–99.

Congalton, R.G., 1991. A review of assessing the accuracy of classifications of remotely sensed data, *Remote Sensing of Environment*, 37:35–46.

Coppin, P.R., and M.E. Bauer, 1996. Digital change detection in forest ecosystems with remote sensing imagery, *Remote Sensing Reviews*, 13:207–234.

Crist, J.B., and R.C. Cicone, 1984. A physically-based transformation of thematic mapper data - the TM tasseled cap, *IEEE Transactions on Geoscience and Remote Sensing*, 22(3):256–263.

Dai, X., and S. Khorram, 1998. The effects of image misregistration on accuracy of remotely sensed change detection, *IEEE Transactions on Geoscience and Remote Sensing*, 36(5):1566–1577.

Ding, Y., C.D. Elvidge, and Ross S. Lunetta., 1998. Survey of multispectral methods for land cover change detection analysis, *Remote Sensing Change Detection: Environmental Monitoring Methods and Applications* (Ross S. Lunetta and Christopher D. Elvidge, editors), Sleeping Bear Press, Inc., New York, N.Y., pp. 21–39.

Elvidge, C.D., and Y. Ding, 1995. Relative radiometric normalization of Landsat multispectral scanner (MSS) data using an automatic scattergram-controlled regression, *Photogrammetric Engineering & Remote Sensing*, 61:1015–1026.

Fung, T., and E. LeDrew, 1988. The determination of optimal threshold levels for change detection using various accuracy indices, *Photogrammetric Engineering & Remote Sensing*, 54:1449–1454.

Gong, P., 1993. Change detection using principal component analysis and fuzzy set theory, *Canadian Journal of Remote Sensing*, 19(1):22–29.

Gong, P., E.F. LeDrew, and J.R. Miller, 1992. Registration noise reduction in difference images for change detection, *International Journal of Remote Sensing*, 13(4):773–779.

Hall, F., D. Strebel, J. Nickeson, and S. Goetz, 1991. Radiometric rectification: Toward a common radiometric response among multidate, multisensor images. *Remote Sensing of Environment*, 35(1):11–27.

Hoffmann, B., 1975. *About Vectors*, Dover Publications, Inc., New York, N.Y., 134 p.

Howarth, P.J., and G.M. Wickware, 1981. Procedures for change detection using Landsat digital data, *International Journal of Remote Sensing*, 2:277–291.

Jensen, J.R., 1996. *Introductory Digital Image Processing: A Remote Sensing Perspective, Second Edition*, Prentice Hall, Upper Saddle River, New Jersey, 316 p.

Jensen, J.R., K. Rutchey, M.S. Koch, and S. Narumalani, 1995. Inland wetland change detection in the Everglades Water Conservation Area 2A using a time series of normalized remotely sensed data, *Photogrammetric Engineering & Remote Sensing*, 61:199–209.

Johnson, R.D., and E.S. Kasischke, 1998. Change vector analysis: A technique for the multispectral monitoring for land cover and condition, *International Journal of Remote Sensing*, 19:411–426.

Lambin, E.F., and A.H. Strahler, 1994a. Change vector analysis in multitemporal space: A tool to detect and categorize land-cover change processes using high temporal-resolution satellite data, *Remote Sensing of Environment*, 48:231–244.

———, 1994b. Indicators of land-cover change for change vector analysis in multitemporal space at coarse spatial scales, *International Journal of Remote Sensing*, 15:2099–2119.

Li, X., and A.G.O. Yeh, 1998. Principal component analysis of stacked multi-temporal images for the monitoring of rapid urban expansion in the Pearl River Delta, *International Journal of Remote Sensing*, 19:1501–1518.

Malila, W.A., 1980. Change vector analysis: an approach for detecting forest changes with Landsat, *Proceedings of the 6th Annual Symposium on Machine Processing of Remotely Sensed Data*, 03-06 June, Purdue University, West Lafayette, Indiana, pp. 326–335.

Mas, J.F., 1999. Monitoring land-cover changes: a comparison of change detection techniques, *International Journal of Remote Sensing*, 20:139–152.

Michalek, J.L., T.W. Wagner, J.J. Luczkovich, and R.W. Stoffle, 1993. Multispectral change vector analysis for monitoring coastal marine environments, *Photogrammetric Engineering & Remote Sensing*, 59:381–384.

Morisette, J.T., and S. Khorram, 2000. Accuracy assessment curves for satellite-based change detection, *Photogrammetric Engineering & Remote Sensing*, 66:875–880.

Nelson, R.F., 1983. Detecting forest canopy change due to insect activity using Landsat MSS, *Photogrammetric Engineering & Remote Sensing*, 49:1303–1314.

Richards, J.A., and X. Jia, 1999. *Remote Sensing Digital Image Analysis, Third Edition*, Springer-Verlag, Berlin, Heidelberg, Germany, 363 p.

Singh, A., 1986. Change detection in the tropical forest of northeastern India using Landsat, *Remote Sensing and Tropical Land Management* (M.J. Eden and J.T. Parry, editors), Chichester Wiley Press, London, United Kingdom, pp. 237–254.

———, 1989. Digital change detection techniques using remotely-sensed data, *International Journal of Remote Sensing*, 10:989–1003.

Smits, Paul C.; and Alessandro Annoni, 2000, Toward specification-driven change detection, *IEEE Transactions on Geoscience and Remote Sensing*, 38(3):1484–1488.

Sohl, T.L., 1999. Change analysis in the United Arab Emirates: An investigation of techniques, *Photogrammetric Engineering & Remote Sensing*, 65:475–484.

Turner II, B.L, D. Skole, Steven Sanderson, Gunther Fischer, Louise Fresco, and Rik Leemans, 1995. *Land-Use and Land-Cover Change Science/Research Plan, IGBP Report No. 35, URL: http://www.geo.ucl.ac.be/LUCC/scienceplan/lucc.html.*

Virag, L.A., and J.E. Colwell, 1987. An improved procedure for analysis of change in Thematic Mapper image-pairs, *Proceedings of the Twenty-First International Symposium on Remote Sensing Environment*, 26-30 October, Ann Arbor, Michigan, pp. 1101–1110.

Weismiller, R.A., S.Y. Kristof, D.K. Scholz, P.E. Anuta, and S.A. Momin, 1977. Change detection in coastal zone environments, *Photogrammetric Engineering & Remote Sensing*, 43:1533–1539.

William, E.R., B.M. William, and B.L. Turner II, 1994. Modeling land use and land cover as part of global environmental change, *Climatic Change*, 28:45–64.

Zhan, X., R. Defries, J.R.G. Townshend, C. Dimiceli, M. Hansen, C. Huang, and R. Sohlbert, 2000. The 250m global land cover change product from the Moderate Resolution Imaging Spectroradiometer of NASA's Earth Observing System, *International Journal of Remote Sensing*, 21:1433–1460.

(Received 07 February 2001; revised and accepted 11 February 2002)